A Fourier Series-Based RLC Interconnect Model for Periodic Signals

Guoqing Chen and Eby G. Friedman
Department of Electrical and Computer Engineering
University of Rochester, Rochester, New York, 14627
guchen,friedman@ece.rochester.edu

***Abstract*— Based on a Fourier series analysis, an analytic interconnect model is presented which is suitable for periodic signals, such as a clock signal. In this model, the far end time domain waveform is approximated by the summation of several sinusoids. Closed form solutions of the 50% delay are provided when the fifth and higher harmonics are ignored. The model is applied to distributed interconnect trees and multiple coupled interconnects. Good accuracy is observed between the model and SPICE simulations. The computational complexity of the model is linear with the number of harmonics.**

I. Introduction

In deep submicrometer integrated circuits, interconnect delay dominates the gate delay. Furthermore, wire inductances can no longer be ignored due to higher signal frequencies and longer wire lengths. Accurate and efficient RLC interconnect models are therefore critical in the design of high performance integrated circuits.

Based on modified Bessel functions, expressions characterizing the transient response of an RLC interconnect have been rigorously developed in [1]. These results, however, are highly complicated and not suitable for an exploratory design process. In order to produce a more efficient solution, the transfer function of the interconnect is truncated and approximated with a few dominant poles, for example, two poles in [2], and four poles in [3]. Four pole expressions are highly accurate, however, no closed form solution has been developed [3]. In all of these models, a step input is assumed and no initial conditions are considered. For a periodic input, if the output signal cannot converge to V_{dd} or 0 within half a period, initial conditions need to be considered. Furthermore, on-chip interconnect often has complicated structures, such as distributed RLC trees and buses. Interconnect models should have the ability to characterize these types of structures.

Fourier analysis has been widely used in RF circuit simulation, where it is named *harmonic balance* [4]. In this paper, Fourier series analysis is applied to digital integrated circuits to model the interconnect behavior. The model is suitable for periodic signals, such as a clock signal. Since the solution is the steady state response, initial conditions are considered. The paper is organized as follows. In section II, the Fourier series-based interconnect model for a single line is presented. In section III, the model is applied to interconnect trees and coupled transmission lines, and the results from the proposed model are compared with SPICE. Finally, some conclusions are offered in Section IV.

This research is supported in part by the Semiconductor Research Corporation under Contract No. 2003-TJ-1068 and 2004-TJ-1207, the National Science Foundation under Contract No. CCR-0304574, the Fulbright Program under Grant No. 87481764, a grant from the New York State Office of Science, Technology & Academic Research to the Center for Advanced Technology in Electronic Imaging Systems, and by grants from Xerox Corporation, IBM Corporation, Intel Corporation, Lucent Technologies Corporation, and Eastman Kodak Company.

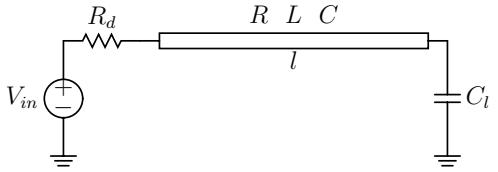

Fig. 1. Equivalent circuit model of a distributed RLC interconnect.

II. Single Interconnect Model

A classical interconnect model is shown in Fig. 1. The interconnect is represented by a distributed RLC transmission line, where l is the interconnect length, and R, L, C are the resistance, inductance, and capacitance per unit length, respectively. The driver is linearized as a voltage source V_{in} serially connected with a driver resistance R_d. The load of the interconnect is modeled as a capacitor C_l.

From the $ABCD$ parameters [5] of a transmission line, the transfer function from V_{in} to the far end of a line is

$$H(s) = \frac{1}{(1 + R_d C_l s)\cosh\theta + (R_d/Z_c + Z_c C_l s)\sinh\theta}, \quad (1)$$

where $\theta = l\sqrt{(R + sL)sC}$ and $Z_c = \sqrt{(R + sL)/sC}$. Since (1) includes hyperbolic functions of the complex frequency s, it is difficult to obtain the time domain solution through an inverse Laplace transform. In order to simplify the problem, the denominator of the transfer function is expanded into an infinite series. By truncating this series, the transfer function is approximated by a few dominant poles [2], [3]. A distributed RLC line can also be modeled by lumped elements through moment matching [6].

In Fig. 2, the transfer function of some existing models [2], [3], [6] are compared with the exact transfer function described in (1). In this example, the interconnect parameters are $l = 2\,\text{mm}$, $R = 8.829\,\text{m}\Omega/\mu\text{m}$, $L = 1.538\,\text{pH}/\mu\text{m}$, and $C = 0.18\,\text{fF}/\mu\text{m}$. The driver resistance and load capacitance are $R_d = 30\,\Omega$ and $C_l = 50\,\text{fF}$, respectively. As illustrated in Fig. 2, a simple L–type lumped model produces the poorest approximation. A two pole model can be accurate up to 5 GHz. A non-uniform two stage L–type lumped model and a four pole model increase the accuracy range to about 7 GHz, however, no closed form solutions for these two models have been reported.

In previous models, the excitation signal is modeled as a step or ramp function, and most of the effort is focused on approximating the transfer function. For a periodic signal, the input signal can be approximated by truncating the Fourier series while maintaining the exact transfer function. The Fourier series representation of a typical

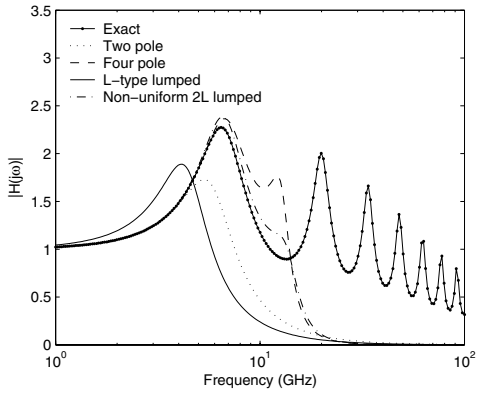

Fig. 2. The amplitude transfer function of different models of an RLC interconnect.

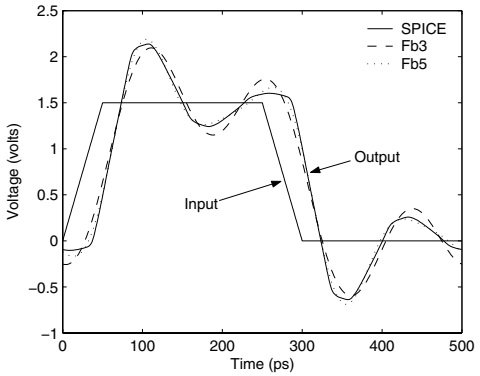

Fig. 3. Comparison of the time domain response of Fb3 and Fb5 with SPICE.

on-chip periodic signal with period T and transition time τ is

$$V_{in}(t) = \frac{V_{dd}}{2} + \sum_{m=1,3,\ldots} A_m \sin(m\omega_0 t + \phi_m), \quad (2)$$

$$\phi_m = -\frac{m\omega_0\tau}{2}, \quad (3)$$

$$A_m = \frac{2TV_{dd}}{\tau m^2\pi^2} \left|\sin\phi_m\right|, \quad (4)$$

where $\omega_0 = 2\pi/T$ is the basis angular frequency, and A_m and ϕ_m are the amplitude and phase of the m^{th} order harmonic, respectively. Since A_m decreases quadratically with m, $V_{in}(t)$ can be approximated by the first several harmonics [7]. The transfer function at each frequency ω can be represented as $H(j\omega) = A(\omega)e^{j\beta(\omega)}$. From (1), the gain of the DC component is $H(0) = 1$. The far end output voltage can be obtained as

$$V_{out}(t) = \frac{V_{dd}}{2} + \sum_{m=1,3,\ldots} A'_m \sin(m\omega_0 t + \phi'_m), \quad (5)$$

where $A'_m = A_m A(m\omega_0)$ and $\phi'_m = \phi_m + \beta(m\omega_0)$. $V_{out}(t)$ can also be approximated by the first several harmonics. In this paper, the Fourier series-based models are referred to as Fb3 and Fb5, with the largest harmonic order number of three and five, respectively. The results from Fb3 and Fb5 are compared with SPICE in Fig. 3. In the SPICE simulation, the interconnect line is divided into 200 segments and each segment is represented by an L–type lumped model. As shown in Fig. 3, two harmonics (Fb3) are sufficient to provide a good approximation of the output voltage waveform for this example.

The 50% delay can be solved numerically from (5). In this paper, the 50% delay is assumed to be less than $T/2 - \tau/2$ (valid in most practical cases). For Fb3, since only two harmonics are considered, a closed form solution is available. In this case,

$$V_{out}(t) \approx \frac{V_{dd}}{2} + A'_1 \sin(\omega_0 t + \phi'_1) + A'_3 \sin(3\omega_0 t + \phi'_3). \quad (6)$$

To determine the 50% delay, (6) is set to $V_{dd}/2$. By applying the multiple-angle formulae, a third order trigonometric expression can be obtained,

$$a_3 x^3 + a_2 x^2 + a_1 x + a_0 = 0, \quad (7)$$

where $x = \tan(\omega_0 t)$ and

$$a_0 = A'_1 \sin\phi'_1 + A'_3 \sin\phi'_3, \quad (8)$$

$$a_1 = A'_1 \cos\phi'_1 + 3A'_3 \cos\phi'_3, \quad (9)$$

$$a_2 = A'_1 \sin\phi'_1 - 3A'_3 \sin\phi'_3, \quad (10)$$

$$a_3 = A'_1 \cos\phi'_1 - A'_3 \cos\phi'_3. \quad (11)$$

A third order expression has either one or three real roots, and a closed form solution exists [8]. If (7) has only one real root x_0, the output waveform crosses $V_{dd}/2$ only once from low-to-high during the first half of a period, and the 50% delay can be expressed as

$$t_d = \frac{\arctan x_0}{\omega_0} - \frac{\tau}{2}. \quad (12)$$

The value of $\arctan x_0$ is in the range of $[0, \pi]$. If (7) has three real roots, the output waveform crosses $V_{dd}/2$ three times during the first half of the period, which means the undershoot point is lower than $V_{dd}/2$. In this case, the output waveform is not shaped like a square wave and can no longer represent logic values.

By setting dV_{out}/dt to zero, the time when the overshoots and undershoots occur can be obtained in the same way as the 50% delay. With these times, the solution of the overshoots and undershoots can be directly determined.

The accuracy of the proposed model depends upon the frequency spectrum of the far end response. For highly LC dominant interconnect, resonance frequencies exist, as shown in Fig. 2. The high order harmonics close to these resonance frequencies are amplified, and the model becomes less accurate. With the signal frequency increasing, the first several harmonics also approach the resonance frequencies and are amplified. The ratio between the harmonics included in the model and the harmonics which are neglected increases, making the proposed model more accurate. The accuracy of the model can be improved by including additional harmonics, and higher order (fifth, seventh, ...) equations should be solved. Since only real roots are of interest, some efficient root-finding algorithms can be used, such as the Newton-Raphson method.

III. Application Examples

The solution for a single distributed RLC line can be readily extended to interconnect trees and multiple coupled interconnects.

A. Distributed interconnect trees

Interconnect trees are widely used in digital integrated circuits, such as clock distribution networks. An example of a distributed RLC tree is shown in Fig. 4, where l_x and C_x are the normalized reference length and capacitance, respectively. All of the branches in the tree are represented by distributed RLC lines.

For a transmission line of length l with load Z_L at the far end, the input impedance seen from the near end is

$$Z_{in} = Z_c \frac{Z_L + Z_c \tanh\theta}{Z_c + Z_L \tanh\theta}, \quad (13)$$

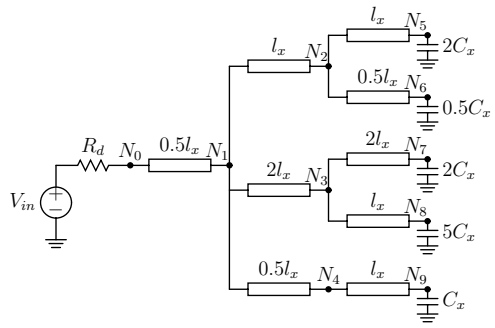

Fig. 4. A distributed RLC tree.

where θ and Z_c are defined in section II. When a node has multiple fanout, the load impedance seen at this node is the parallel combination of the input impedance of the downstream branches. The transfer function from N_0 to a certain node N_i is the product of the transfer function of all of the branches along the unique path from N_0 to N_i. The transfer function of a single branch can be obtained by replacing R_d by 0 and $C_l s$ by $1/Z_L$ in (1),

$$H(s) = \frac{1}{\cosh\theta + (Z_c/Z_L)\sinh\theta}. \tag{14}$$

The transfer function from the voltage source to a certain node N_i, therefore, is

$$H_i(s) = \frac{Z_{L,0}}{R_d + Z_{L,0}} \prod_k \frac{1}{\cosh\theta_k + (Z_{c,k}/Z_{L,k})\sinh\theta_k}, \tag{15}$$

where $Z_{L,0}$ is the input impedance seen from N_0, and k is the index covering each branch in the path from N_0 to N_i. From this analysis, the computational complexity required to determine the time domain response is linear with the size of the tree and the number of harmonics.

The branches in the tree shown in Fig. 4 can have different parasitic interconnect impedances. For simplicity, the branches are assumed to be the same width, 6 μm. Ground wires are placed at each side of the signal line as shields. The width of the shield wire is 10 μm and the space between the shield and the clock line is 6 μm. The interconnect parameters of such a structure are $R = 3.9\,\text{m}\Omega/\mu\text{m}$, $L = 0.43\,\text{pH}/\mu\text{m}$, and $C = 0.36\,\text{fF}/\mu\text{m}$.

A 2 GHz clock signal with $\tau = 50\,\text{ps}$ is applied at the input of the tree. The 50% delay at node $N5$ and $N7$ is listed in Table I for a range of circuit parameters. To drive the interconnect tree with a high frequency signal, the driver resistance has to be sufficiently small. Results from the two pole model [2] and the equivalent Elmore delay model [9] are, for comparison, also listed.

The methods presented in [2] and [9] have similar accuracy and complexity, since both of these models are based on second order approximations. As listed in Table I, Fb3 and Fb5 produce higher accuracy, for this example, than the second order approximations. The average error of Fb5 is only 3%. The accuracy of the Fourier series based model can be enhanced to capture the fine details of the waveform by including additional harmonics, and there are no stability and numerical problems such as suffered by AWE [10].

B. Multiconductor Systems

For multiple transmission lines, the interconnect parameters per unit length can be represented by matrices $\boldsymbol{R}$, $\boldsymbol{L}$, and $\boldsymbol{C}$. All of these matrices are symmetric with the dimension $N \times N$, where N is the number of lines. From the Telegrapher equations of N coupled

TABLE I

50% DELAY AT NODES $N5$ AND $N7$ FROM Fb3 AND Fb5 AS COMPARED WITH THE RESULTS FROM SPICE AND SECOND ORDER MODELS.

lx (mm)	R_d (Ω)	C_x (fF)	Node	SPICE (ps)	[2] (ps)	[9] (ps)	Fb3 (ps)	Fb5 (ps)
0.2	10	20	$N5$	13.1	10.3	10.2	9.0	10.3
0.2	10	20	$N7$	11.6	14.0	13.8	10.6	11.2
0.2	10	500	$N5$	35.5	50.0	49.1	49.0	37.1
0.2	10	500	$N7$	59.9	60.8	58.6	60.1	60.0
0.2	30	20	$N5$	23.9	23.6	23.5	25.1	24.1
0.2	30	20	$N7$	23.5	25.6	25.4	25.7	24.5
0.2	30	100	$N5$	42.7	40.0	39.8	43.2	42.1
0.2	30	100	$N7$	39.4	43.1	42.5	44.1	41.2
1	10	20	$N5$	41.3	54.3	52.2	37.0	40.8
1	10	20	$N7$	75.8	79.7	75.1	77.5	75.3
1	10	100	$N5$	51.3	63.3	60.4	49.9	52.4
1	10	100	$N7$	89.6	93.0	86.9	89.6	89.2
1	20	20	$N5$	49.2	71.3	68.6	48.4	48.3
1	20	20	$N7$	86.4	96.1	89.4	90.6	88.1
1	20	100	$N5$	57.4	85.1	81.7	57.7	58.8
1	20	100	$N7$	104.1	114.0	105.4	103.4	102.9
Maximum Error					48%	42%	38%	21%
Average Error					18%	15%	8%	3%

transmission lines, the voltage vector $\boldsymbol{V}$ and current vector $\boldsymbol{I}$ have the following relationship in the frequency domain,

$$\frac{\partial}{\partial x}\begin{pmatrix} \boldsymbol{V} \\ \boldsymbol{I} \end{pmatrix} = -\begin{pmatrix} \boldsymbol{0} & \boldsymbol{Z} \\ \boldsymbol{Y} & \boldsymbol{0} \end{pmatrix}\begin{pmatrix} \boldsymbol{V} \\ \boldsymbol{I} \end{pmatrix}, \tag{16}$$

where $\boldsymbol{Z} = \boldsymbol{R} + s\boldsymbol{L}$ and $\boldsymbol{Y} = s\boldsymbol{C}$.

The matrix $\boldsymbol{ZY}$ for a practical system is always diagonalizable [11], *i.e.*, $\boldsymbol{ZY} = \boldsymbol{MQM}^{-1}$, where $\boldsymbol{Q}$ is a diagonal matrix with eigenvalues of $\boldsymbol{ZY}$ as the diagonal elements, and matrix $\boldsymbol{M}$ has the corresponding eigenvectors of $\boldsymbol{ZY}$ as the columns. Decoupling (16) can be achieved by applying a modal analysis [11], [12],

$$\frac{\partial}{\partial x}\begin{pmatrix} \hat{\boldsymbol{V}} \\ \hat{\boldsymbol{I}} \end{pmatrix} = -\begin{pmatrix} \boldsymbol{0} & \hat{\boldsymbol{Z}} \\ \hat{\boldsymbol{Y}} & \boldsymbol{0} \end{pmatrix}\begin{pmatrix} \hat{\boldsymbol{V}} \\ \hat{\boldsymbol{I}} \end{pmatrix}, \tag{17}$$

where $\hat{\boldsymbol{V}} = \boldsymbol{M}^{-1}\boldsymbol{V}$, $\hat{\boldsymbol{I}} = \boldsymbol{M}^T\boldsymbol{I}$, $\hat{\boldsymbol{Z}} = \boldsymbol{M}^{-1}\boldsymbol{Z}(\boldsymbol{M}^T)^{-1}$, and $\hat{\boldsymbol{Y}} = \boldsymbol{M}^T\boldsymbol{Y}\boldsymbol{M}$. Since $\boldsymbol{Z}$ and $\boldsymbol{Y}$ are symmetric, $\hat{\boldsymbol{Z}}$ and $\hat{\boldsymbol{Y}}$ are both diagonal [12]. The N coupled interconnect lines, therefore, are decoupled into N independent lines. The characteristic impedance matrix $\hat{\boldsymbol{Z}}_c$ and the propagation coefficient matrix $\hat{\boldsymbol{\gamma}}$ of the decoupled system are $\hat{\boldsymbol{Z}}_c = \sqrt{\hat{\boldsymbol{Z}}\hat{\boldsymbol{Y}}^{-1}} = \text{diag}(\hat{Z}_{c,1}, \hat{Z}_{c,2}, \ldots, \hat{Z}_{c,N})$ and $\hat{\boldsymbol{\gamma}} = \sqrt{\hat{\boldsymbol{Z}}\hat{\boldsymbol{Y}}} = \text{diag}(\hat{\gamma}_1, \hat{\gamma}_2, \ldots, \hat{\gamma}_N)$, respectively.

This decoupling method has been extended to drivers and loads in [8] and [13] for two and more interconnects. These extensions, however, are only suitable for identical lines with identical drivers and loads. Furthermore, the inductance matrix in [13] is obtained as $\boldsymbol{L} = \boldsymbol{C}^{-1}/v^2$, where v is the speed of light in a dielectric. This expression is valid only for a homogeneous dielectric with an ideal ground for the current return path. With these constraints, the practical generality of these models is greatly limited.

The $ABCD$ matrices of the decoupled transmission lines are [5] $\hat{\boldsymbol{A}}_p = \text{diag}\ (\cosh\hat{\gamma}_k)$, $\hat{\boldsymbol{B}}_p = \text{diag}\ (\hat{Z}_{c,k}\sinh\hat{\gamma}_k)$, $\hat{\boldsymbol{C}}_p = \text{diag}\ (\sinh\hat{\gamma}_k/\hat{Z}_{c,k})$, and $\hat{\boldsymbol{D}}_p = \text{diag}\ (\cosh\hat{\gamma}_k)$, where $k = 1, 2, \ldots, N$. The boundary conditions of the N coupled lines are

$$\boldsymbol{V}_d = \boldsymbol{V}_{in} - \boldsymbol{R}_d\boldsymbol{I}_d, \tag{18}$$

$$\boldsymbol{I}_r = s\boldsymbol{C}_l\boldsymbol{V}_r, \tag{19}$$

where $\boldsymbol{R}_d$ and $\boldsymbol{C}_l$ are, respectively, the driver resistance matrix and load capacitance matrix, both of which are diagonal. The subscript

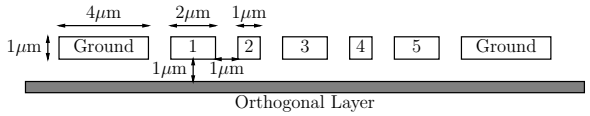

Fig. 5. Geometric characteristics of a five line system.

d and r represent the driver side (or near end) and receiver side (or far end), respectively. After some mathematical simplification, the transfer function matrix is

$$\boldsymbol{H} = (\boldsymbol{R}_d\boldsymbol{C}_p + s\boldsymbol{R}_d\boldsymbol{D}_p\boldsymbol{C}_l + \boldsymbol{A}_p + s\boldsymbol{B}_p\boldsymbol{C}_l)^{-1}. \quad (20)$$

The $ABCD$ matrices of the coupled transmission lines are

$$\boldsymbol{A}_p = \boldsymbol{M}\hat{\boldsymbol{A}}_p\boldsymbol{M}^{-1}, \quad (21)$$

$$\boldsymbol{B}_p = \boldsymbol{M}\hat{\boldsymbol{B}}_p\boldsymbol{M}^{T}, \quad (22)$$

$$\boldsymbol{C}_p = (\boldsymbol{M}^{T})^{-1}\hat{\boldsymbol{C}}_p\boldsymbol{M}^{-1}, \quad (23)$$

$$\boldsymbol{D}_p = (\boldsymbol{M}^{T})^{-1}\hat{\boldsymbol{A}}_p\boldsymbol{M}^{T}. \quad (24)$$

In general, $\boldsymbol{M}$ is a matrix function of s and cannot be expressed in closed form [11]. Furthermore, the matrix inverse operation in (20) does not permit an analytic expression (or an analytic low order approximation) of the transfer function to be obtained. Conventional inverse Laplace transform based methods [1]–[3], which assume a step or ramp input, can no longer be used. The proposed model, which assumes a periodic input signal, remains valid, since the solution of (20) is only required at certain discrete frequencies (*e.g.*, the harmonic frequencies of the input signal), and can be solved numerically at each frequency. When N is less than five, closed form solutions exist [13] to calculate $\boldsymbol{M}$ and $\boldsymbol{Q}$. For larger N, numerical methods have to be used, and the computing complexity increases. When $s = 0$, $\boldsymbol{H}$ becomes an identity matrix. Since no approximation is made in this derivation, (20) is the exact transfer function of a coupled multi-conductor system. Upon obtaining the transfer coefficient at each harmonic frequency, the output signal can be determined in the same way as in (5). In this multiconductor model, no constraints are made on the interconnect parameters, making the solution of general use.

The physical geometry of a five line system is shown in Fig. 5. Ground lines are placed on each side of the signal lines to provide current return paths. Without loss of generality, capacitive coupling is assumed to exist only between adjacent lines and $\boldsymbol{R}$ is assumed to be diagonal. In this example, the driver and load are $\boldsymbol{R}_d = \mathrm{diag}(50, 30, 40, 50, 30)\,\Omega$, and $\boldsymbol{C}_l = \mathrm{diag}(50, 100, 80, 80, 50)$ fF, respectively. Only one aggressor is considered and the multi-aggressor problem can be solved by applying superposition. The maximum crosstalk noise determined by the Fourier series-based model is compared with SPICE in Table II. In the experiments, line 1 is the aggressor, and all of the other lines are quiet victims (represented as V2 to V5 in Table II). As shown in Table II, Fb3 provides limited accuracy in multi-conductor systems. This result is not surprising, since the magnitude of the transfer function of the victims is small at low frequencies (zero at DC). Thus, the high frequency components are comparable or greater than the low frequency components at the output, and are therefore not negligible. By including one additional harmonic, Fb5 provides greater accuracy, exhibiting an average error of 8.4%. Note that the proposed model is more accurate for nearby victims.

TABLE II

COMPARISON OF THE MAXIMUM CROSSTALK NOISE OF Fb3 AND Fb5 WITH SPICE SIMULATIONS. THE INPUT SIGNAL PARAMETERS ARE $T = 500$ ps, $\tau = 50$ ps, AND $V_{dd} = 1.5$ volts.

l (mm)	Victim	SPICE (mV)	Fb3 (mV)	Fb3 % Error	Fb5 (mV)	Fb5 % Error
2	V2	155.9	131.4	15.7	151.9	2.6
	V3	67.6	48.9	27.7	69.8	3.3
	V4	54.6	39.3	28.0	57.5	5.3
	V5	40.6	26.8	34.0	40.9	0.7
4	V2	190.5	197.0	3.4	195.2	2.5
	V3	68.8	73.4	6.7	62.0	9.9
	V4	60.3	54.4	9.8	54.0	10.4
	V5	48.2	38.4	20.3	34.7	28.0
6	V2	188.8	201.8	6.9	192.4	1.9
	V3	110.6	79.6	28.0	99.0	10.5
	V4	95.0	66.7	29.8	87.4	8.0
	V5	74.0	43.9	40.7	60.9	17.7

IV. CONCLUSIONS

By exploiting a Fourier series representation of a typical on-chip signal, an analytic time-domain solution for an RLC interconnect is shown to be an effective modeling strategy. Closed form solutions of the 50% delay are presented. The model is applied to distributed interconnect trees and multiple coupled interconnects, the transfer functions of which are exact. Good accuracy is observed between the proposed model and SPICE simulations.

REFERENCES

[1] J. A. Davis and J. D. Meindl, "Compact Distributed RLC Interconnect Models–Part I: Single Line Transient, Time Delay, and Overshoot Expressions," *IEEE Transactions on Electron Devices*, Vol. 47, No. 11, pp. 2068–2077, November 2000.

[2] A. B. Kahng and S. Muddu, "An Analytical Delay Model for RLC Interconnects," *IEEE Transactions on Computer-Aided Design of Integrated Circuits and Systems*, Vol. 16, No. 12, pp. 1507–1514, December 1997.

[3] K. Banerjee and A. Mehrotra, "Accurate Analysis of On-Chip Inductance Effects and Implications for Optimal Repeater Insertion and Technology Scaling," *Proceedings of the IEEE Symposium on VLSI Circuits*, pp. 195–198, June 2001.

[4] K. S. Kundert, "Introduction to RF Simulation and Its Application," *IEEE Journal of Solid-State Circuits*, Vol. 34, No. 9, pp. 1298–1319, September 1999.

[5] L. N. Dworsky, *Modern Transmission Line Theory And Applications*, John Wiley & Sons, NY, 1979.

[6] A. B. Kahng and S. Muddu, "Optimal Equivalent Circuits for Interconnect Delay Calculations Using Moments," *Proceedings of the European Design Automation Conference*, pp. 164–169, September 1994.

[7] K. T. Tang and E. G. Friedman, "Lumped Versus Distributed RC and RLC Interconnect Impedance," *Proceedings of the IEEE Midwest Symposium on Circuits and Systems*, pp. 136–139, August 2000.

[8] L. Yin and L. He, "An Efficient Analytical Model of Coupled On-Chip RLC Interconnects," *Proceedings of the IEEE Design Automation Conference – Asian and South Pacific*, pp. 385–390, January 2001.

[9] Y. Ismail, E. G. Friedman, and J. L. Neves, "Equivalent Elmore Delay for RLC Trees," *IEEE Transactions on Computer-Aided Design of Integrated Circuits and Systems*, Vol. 19, No. 1, pp. 83–97, January 2000.

[10] L. T. Pillage and R. A. Rohrer, "Asymptotic Waveform Evaluation for Timing Analysis," *IEEE Transactions on Computer-Aided Design of Integrated Circuits and Systems*, Vol. 9, No. 4, pp. 352–366, April 1990.

[11] S. Lin and E. Kuh, "Transient Simulation of Lossy Interconnects Based on the Recursive Convolution Formulation," *IEEE Transactions on Circuits and System*, Vol. 39, No. 11, pp. 879–892, November 1992.

[12] F. Romeo and M. Santomauro, "Time-Domain Simulation of N Coupled Transmission Lines," *IEEE Transactions on Microwave Theory and Technology*, Vol. 35, No. 2, pp. 131–137, February 1987.

[13] J. Chen and L. He, "A Decoupling Method for Analysis of Coupled RLC Interconnects," *Proceedings of the ACM Great Lakes Symposium on VLSI*, pp. 41–46, April 2002.